2017-02

A systematic approach to determining the minimum sampling rate for real-time spacecraft control

Zappulla, Richard II; Romano, Marcello

To appear in the proceedings of the 27th AAS/AIAA Spaceflight Mechanics Meeting, San Antonio, TX
February 6-9, 2017

AAS 17-424

A SYSTEMATIC APPROACH TO DETERMINING THE MINIMUM SAMPLING RATE FOR REAL-TIME SPACECRAFT CONTROL

Richard Zappulla II[*] and Marcello Romano[†]

Typical controller design and analysis methods utilize techniques for continuous-time systems. However, digital computation is the favored approach to implementing the resulting controllers. This leads to the natural question of choosing an appropriate sampling rate for the controller. There exist several "Rules of Thumbs" for choosing a sample rate derived from primarily frequency domain properties of the system. A metric to estimate the sample rate based on the system properties rooted from first principles is developed. It is then validated via several case studies using representative mechanical systems, actuators, and controllers. Lastly, the paper concludes with a discussion on the applications of this metric.

INTRODUCTION

Traditional control design and analysis methods are built the ability to express both the system dynamics and controller outputs as a continuous-time function. The resulting controllers using design typical methods such as Root Locus, Bode analysis and Lyapunov analysis are then typically implemented digitally. To operate, a digital control system samples, typically at a fixed interval, the current state of the continuous system to generate a reference trajectory. From there, the sampled state and reference trajectory are then utilized by a controller to generate a desired control input sends the command to an actuator to control the system. Generally, the faster a digital control system performs this process, the more effectively it can compensate for variations in model parameters, unmodeled effects, and sensor noise.[1] However, as the rate of the digital controller increases, so does the computational burden placed on the computational architecture (i.e. processor, memory, PCI-bus, etc.). This naturally leads to the question, *at what rate does the controller need to run to achieve a desired level of performance?*. In general, the minimum sampling rate for the GNC system is influenced by numerous factors, such as, the 'speed' of the underlying dynamics, acceptable error tolerances, computational limitations, actuator strength, vehicle physical properties (i.e. mass and inertia), ability to effectively track a commanded control input, sensitivity to uncertainties in plant parameters and measurement noise, as well as other external factors, such as safety.[1]

To aid in determining the minimum sampling rate, there exists multiple "Rules of Thumb" based on engineering experience. One such rule of thumb states the minimum sampling rate should be at least 10 times larger than the system bandwidth. Rules such as this are predicated on Euler's Approximation; that is, for a small enough time step, the non-zero discrete derivative sufficently approximates the continuous derivative.[2] Note, this time step is dependent upon the controller formulation (e.g. PD, Lead-Lag, etc) and the response of the system to a given input (e.g. step input, si-

[*]PhD Candidate, Mechanical and Aerospace Department, Naval Postgraduate School, 1 University Circle, Monterey CA 93940

[†]Associate Professor, Mechanical and Aerospace Department, Naval Postgraduate School.

nusoidal input, etc). For responses containing significant higher frequency components, the sample time must be small in order to capture the these short period fluctuations. Another common metric which can be used in determining the minimum sampling rate is the Nyquist Sampling Theorem, which states the minimum sampling rate must be twice the frequency of the highest frequency of interest. For spacecraft, these frequencies of interest are those up to and including the system bandwidth. It is worthwhile to note, these rules of thumb are based on frequency domain properties of the system, which are only defined for linear systems.[3,4] Lastly, the maximum sampling period can be estimated by examining the Lipschitz constant of the system. Specifically, the maximum sampling period for a system is one whose inverse is greater than or equal to the Lipschitz frequency (i.e. Lipschitz constant) for the system. However, determining the Lipschitz constant is not trivial and requires *a priori* knowledge of the control input to the system and its response.[5–7] As suggested by Ross, one such approximation method to estimate the Lipschitz frequency is to vary the sample and hold time of a controller in a numerical simulation and assess the stability of the resulting system.[6,7] To the best of authors' knowledge, no other metrics or methodologies for suggesting a minimum sampling rate for the real-time control of a mechanical system has been proposed in literature which utilize physical properties of the system and is rooted in first principles.

Motivated by this, a methodology was developed systematically from first principles, utilizing the system properties, to estimate the minimum sampling rate necessary for the guidance and/or control subsystems to achieve a desired performance. Several relevant (numerical) case studies are performed using representative mechanical systems, actuators, and controllers to validate this metric. The remainder of the paper is as follows: the minimum sampling rate metric is first developed. Next, the metric is validated via numerical simulations using representative mechanical systems including a three-axis spacecraft reorientation maneuver using an Eigenaxis-Quaternion feedback controller, a simple harmonic oscillator with a PD controller, and the minimum-time control of a double-integrator system using reaction control jets. Lastly, the paper will conclude with a discussion on the application of this metric to the design of software and the selection of hardware.

MINIMUM SAMPLING RATE FORMULATION

Modern controllers are designed and analyzed in the continuous-time domain and implemented, however, in a discrete manner via a digital computer, typically at a fixed interval, T_c. The use of a digital computer fundamentally implies a non-zero delay to computational delay, Δt_c, associated with sensor acquisition and computation of the control input. This further implies the control output is held constant over the next computational period. Furthermore, actuators typically realize the control input through the conversion of a digital commanded input to an analog signal via a digital-to-analog conversion. As a result of this quantization process, the output of the actuator is limited to discrete levels between zero to it maximum output. Exploiting these inherent features of a physical system, a minimum sampling rate metric can be derived from first principles.

Consider first the generic model for a nonlinear system,

$$\dot{x}(t) = f(x(t), u(t), t) \tag{1}$$

Over short the period over which the actuator output remains constant, the motion of a mechanical system is assumed to be sufficiently described as rectilinear motion. As a result, the time-averaged acceleration can be written as,

$$\frac{\dot{x}\left(t + \Delta t_c\right) - \dot{x}(t)}{\Delta t_c} = \frac{1}{\Delta t_c} \int_t^{t+\Delta t_c} u(\tau)\, d\tau \tag{2}$$

where $u(\tau)$ is the control input. Note, the first order difference equation in Eq. (2) approaches the derivative ${}^{d\dot{x}}/_{dt} = u$ in the limit as $\Delta t_c \to 0$. Rewritting Eq. (2) as,

$$\Delta \dot{x} = u(t)\Delta t_c \tag{3}$$

implies a minimum acceleration impulse which can be imparted onto the system.

Before continuing, it is worth noting, in the context of defining real-time for a system, the acceleration term can be interpreted as a *dynamic bandwidth*, ζ_{BW}. The dynamic bandwidth is defined as,

$$\zeta_{\text{BW}} = \frac{\text{Minimum Control Resolution}}{\text{Appropriate Physical Quantity}} \tag{4}$$

Analogous to a system bandwidth, ω_{BW}, the dynamic bandwidth is a system-level metric which can be used to provide insight into the responsiveness of the system. However, unlike the system bandwidth which is typically considered to be inversely proportional to the maximum responsiveness of the system, the dynamic bandwidth captures the minimum responsiveness of the system.[3] Additionally, while the system bandwidth is only formally defined for linear systems, the dynamic bandwidth is defined for both linear and nonlinear systems.[3,4]

Continuing, Eq. (**??**) implies a corresponding change in the state of the system which can be written in terms of the dynamic bandwidth as,

$$x\left(t + \Delta t_c\right) - x(t) = \Delta x = \frac{1}{2}\zeta_{\text{BW}}\Delta t_c^2 \tag{5}$$

Furthermore, given an acceptable change in state (i.e. error) and dynamic bandwidth for a particular application, the maximum sampling time, T_{RT}, which captures the dynamics of the system can be estimated as,

$$T_{\text{RT}} = \frac{1}{2}\sqrt{\frac{2\Delta x}{\zeta_{\text{BW}}}} \tag{6}$$

Therefore, the resulting minimum sampling rate, f_{RT} for a control system to be considered real-time is

$$f_{\text{RT}} = 2\sqrt{\frac{\zeta_{\text{BW}}}{2\Delta x}} \tag{7}$$

Both the maximum sampling period and minimum sampling rate metrics proposed in Eq. (6) and Eq. (7) respectively have several implications. First, both metrics are bounded by the physical system (i.e. mass, inertial , actuator strength) as well as the control system implementation. The proposed metrics provide insights into the system which are easily mapped to the physical system. Furthermore, these metrics provide the designer with 'knobs' they can adjust in order to estimate the affects of changes on various aspects of the system.

NUMERICAL CASE STUDIES

To aid in the validation of this metric, several numerical case studies are performed using representative mechanical systems, controllers, and actuators with discrete output levels. The systems considered include a three-axis reorientation maneuver of a spacecraft using reaction wheels and an Eigenaxis-Quaternion feedback controller;[8,9] a simple harmonic oscillator with a PD controller;[3,4] and a double integrator (DI) system with reaction control jets using the minimum-time optimal control policy.[10] All of these controllers, with the exception of the minimum-time control policy for

a double integrator system, have been shown to be stable in literature. For an implementation of the minimum time control policy with a sample time $T_s > 0$, the system will spend most of the time operating off of the switching curve. A stability assessment of the control policy while off the switching curve is presented in the Appendix.

Numerical Case Study Results

Unless otherwise specified, the mass of the system was chosen to be unity for simplicity. Each actuator is assumed to have a maximum control output of of unity and a resolution of 0.001, except for the reaction jets which is a purely discrete actuator with two states: ON or OFF. Additionally, each system was tuned to settle within 60 seconds and achieve stability with a delay of 1 second. Furthermore, each system utilizes continuous dynamics propagated using a variable step solver and a controller which is sampled with a fixed period, T_s. The controller sampling period was varied between 0.001 seconds (1 kHz) to 1 second (1 Hz). Each scenario was run for 120 seconds and the average steady-state error in x was recorded over the last 60 seconds. The results of each case study were then compared with the predicted minimum change in state given by Eq. (5). To further aid in comparison, the dynamic bandwidth in Eq. (5) is replaced with the second-order equivalent system bandwidth, $\omega_{\text{BW}}^2 = {}^{k}/_{m}$ and the result is presented.

Overall System Responses The combined responses of each system are illustrated together in Figure 1. Each system was found to exhibit a log-linear response in the average minimum change in the state x compared to the sampling rate. Additionally, in order to reduce the numerical noise and increase clarity, each response was curve-fit to a log-linear response. This response, and its estimated 1σ error are illustrated in subsequent figures to further highlight the trends of various responses.

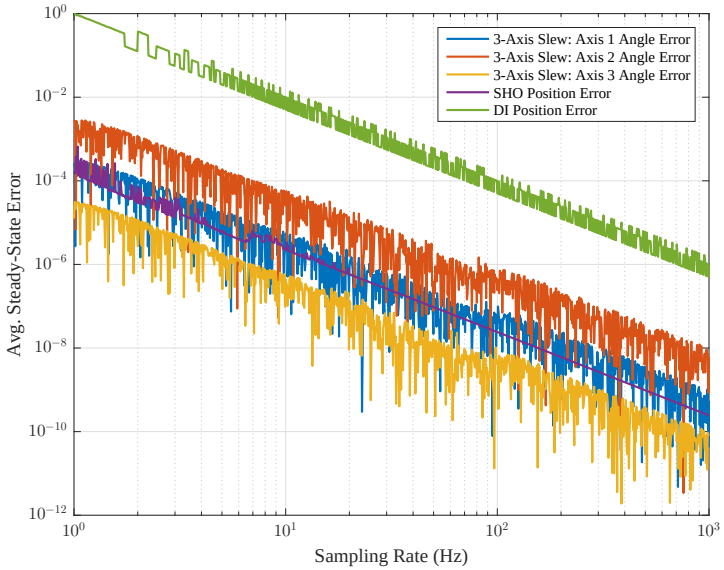

Figure 1. Average Steady-State Error versus Controller Sample Time

Eigenaxis-Quaternion Feedback Controller The first case considered is a three-axis reorientation maneuver of spacecraft using an Eigenaxis-Quaternion feedback controller. Additionally, to produce the torque, a set of 3 orthogonal reaction wheels were modeled and placed in the loop This system is relevant as it is nonlinear in both the system dynamics and control. The system dynamics

are governed by Euler's Equation and given as,

$$\boldsymbol{\tau} = \mathbf{J}\dot{\boldsymbol{\omega}} + \boldsymbol{\omega}^{x}\mathbf{J}\boldsymbol{\omega} \tag{8}$$

where $\boldsymbol{\tau}$ is the control torque, $\mathbf{J}$ is the inertia matrix about the center of mass in the spacecraft body-frame, $\boldsymbol{\omega}$ is the angular velocity of the spacecraft, and $\boldsymbol{\omega}^{x}$ is the matricial representation of the cross product operator.[9] Additionally, the Eigenaxis-Quaternion feedback controller is given as,

$$\mathbf{u}(t) = -2k\eta_{\text{err}}\mathbf{J}\boldsymbol{\varepsilon}_{\text{err}} - c\mathbf{J}\boldsymbol{\omega}_{\text{err}} + \boldsymbol{\omega}^{x}_{\text{err}}\mathbf{J}\boldsymbol{\omega}_{\text{err}} \tag{9}$$

where $\boldsymbol{\varepsilon}_{\text{error}} \in \mathbb{R}^3$ is a column vector containing the vector components of the error quaternion , $\eta_{\text{error}} \in \mathbb{R}$ is the scalar component of the error quaternion, and the scalar gains $c, k \in \mathbb{R}_+$. The stability of this controller was proven via Lyanpunov's Direct method.[8,9] Lastly, the error angle was defined as.,[9]

$$\theta_{\text{error}} = 2\cos^{-1}\left(\eta_{\text{error}}\right) \tag{10}$$

In order to examine the effect of various physical properties, the inertia matrix was chosen to be $\mathbf{J} = \text{diag}(1, 0.1, 10)$. Additionally, to meet the 60-second settling time, the scalar gains were chosen to be $k = 0.3$ and $c = 1.0$. The results from the case study are presented in Figure 2. When compared to the response of the system, the dynamic bandwidth closely matches the first-order fitted response of the numerical experiment. Additionally, the dynamic bandwidth was observed to maintain a similar level of error as the inertia was varied between the three axes. Lastly, the predicted minimum sampling rate associated with using the system bandwidth and dynamic bandwidth both over predict the minimum sampling rate in order to achieve a specific error level. The prediction associated with the dynamic bandwidth estimate is within an order of magnitude as the numerical response compared to using the system bandwidth metric. For this particular case, the predicted error for a given sample time agrees very well with the numerical experiment.

Simple Harmonic Oscillator with PD Control The second case considered is a simple harmonic oscillator (SHO) with a PD controller. The dynamics of a SHO are given as,

$$\ddot{x} = -\frac{k}{m}x \tag{11}$$

where $k \in \mathbb{R}_+$ and is typically referred to as the spring constant for a mechanical system.[3,4] This is a representative second-order system with a common controller. As illustrated in Figure 3 the dynamic bandwidth sufficiently estimates the sample time required to achieve a desired level of system performance. Similar to the first case, both metrics over-predict the sampling rate necessary to achieve a given level of steady-state error. Likewise, the prediction associated with the dynamic bandwidth is smaller than that associated with the system bandwidth and is within an order of magnitude of the average numerical response.

Minimum-Time Optimal Control for a Double Integrator System The third case study considered is a double integrator (DI) system under a minimum-time optimal control policy using discrete actuators, such as reaction jets. There are two primary methods of implementing this particular control policy. The first method is a clock-based method which assumes knowledge of the switching time. The second method - the method implemented for this case study - involves the use of a full-state switching curve, given in Eq. (19) , to determine the switching point. As illustrated by Figure 4, the dynamic bandwidth sufficiently estimates the predicted steady-state error given a sampling time. Note, since the system bandwidth and dynamic bandwidth are the same numerically, both methods produce the same prediction. Lastly, compared to the SHO, the DI system with discrete actuators produces substantially more variation in the steady-state error.

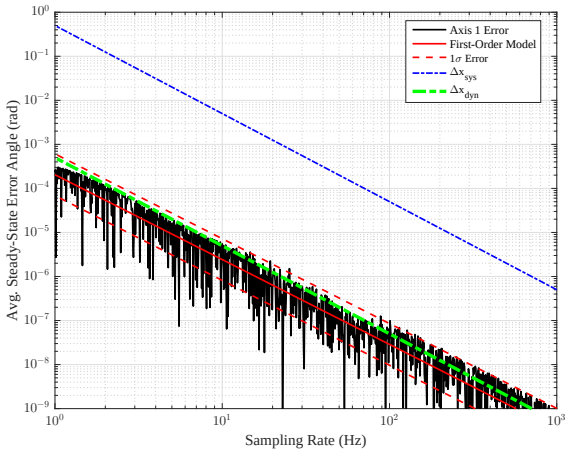

(a) Axis 1:($J_{11} = 1\,\mathrm{kg\,m^2}$)

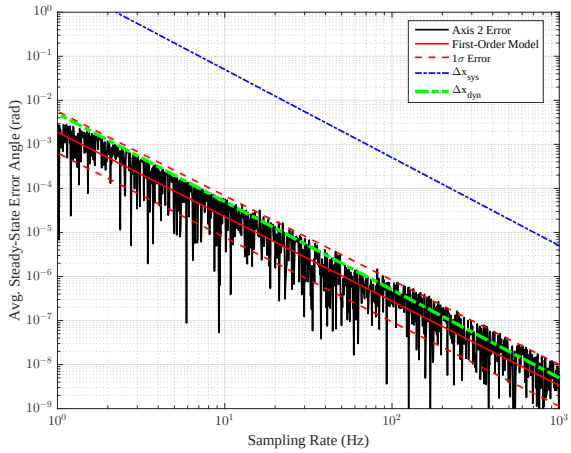

(b) Axis 2: ($J_{22} = 0.1\,\mathrm{kg\,m^2}$)

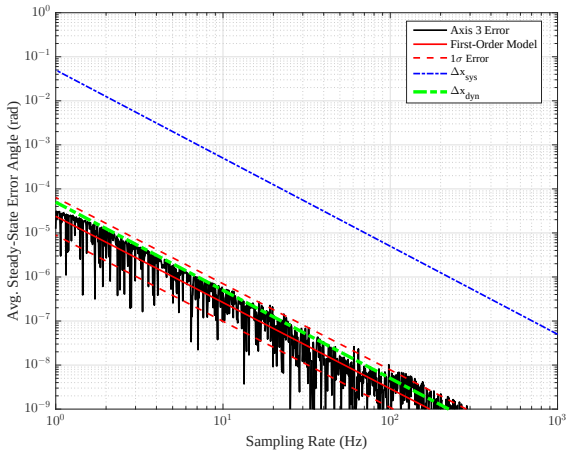

(c) Axis 3: ($J_{33} = 10\,\mathrm{kg\,m^2}$)

Figure 2. Average Steady-State Error Versus Controller Sample Time for a 3-Axis Spacecraft Reorientation maneuver

APPLICATIONS AND DISCUSSION

Minimum Sampling Rate for Tracking Transient Responses

As demonstrated, this metric provides an order of magnitude estimate for the sampling rate required to track a control signal to within a specified level of error. The dynamic bandwidth as given in Eq. (4) provides the lower-bound on the steady-state tracking capability of the system. Redefining the dynamic bandwidth to be equivalent to the maximum acceleration of the system,

$$\zeta_{\mathrm{BW}} = \frac{\text{Maximum Control Effort}}{\text{Appropriate Physical Quantity}} \tag{12}$$

one can upper bound the transient tracking capability of the system. Rewriting Eq. (3) and substituting in Eq. (12), the maximum sampling time T_{RT} and minimum sampling rate f_{RT} can be upper-bounded respectively as,

$$T_{\mathrm{RT}} = \frac{1}{f_{\mathrm{RT}}} = \frac{\Delta\dot{x}_{\max}}{\zeta_{\mathrm{BW}}} \tag{13}$$

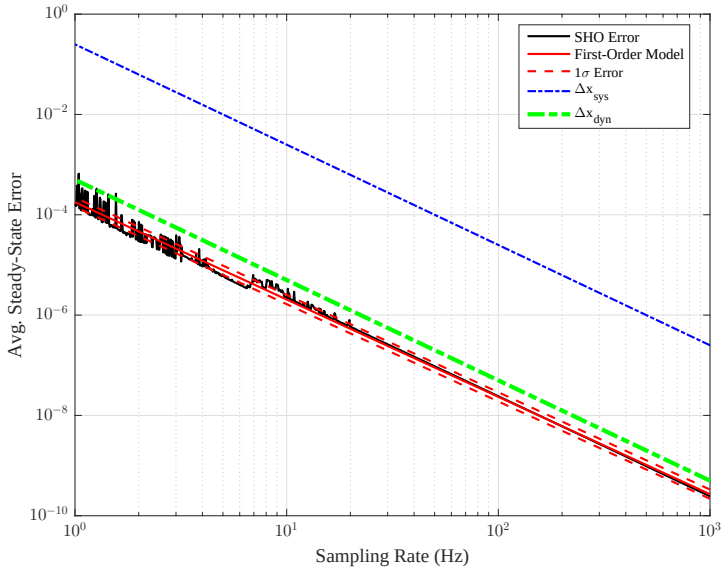

Figure 3. Average Steady-State Error Versus Controller Sample Time for a Simple Harmonic Oscillator

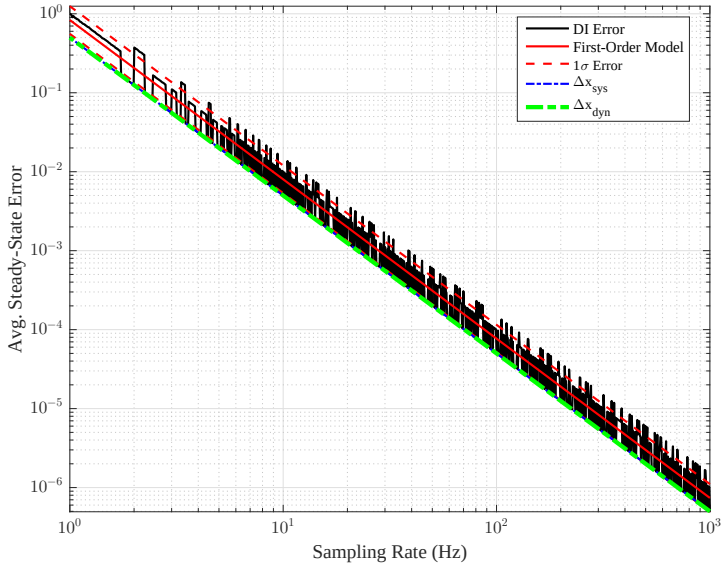

Figure 4. Average Steady-State Error Versus Controller Sample Time for a Double-Integrator System Under the Minimum-Time Optimal Control Policy

For example, consider the maximum change in error, $^{\Delta x_{err}}/_{\Delta t_c}$, of the previously exmained SHO system during its transient period consisting of the first 60 seconds. As illustrated by Figure 5, the dynamic bandwidth provides an estimated sampling rate to within 36% of the response of the system, while the system bandwidth significantly underestimates the required sampling rate to achieve a desired level of tracking error.

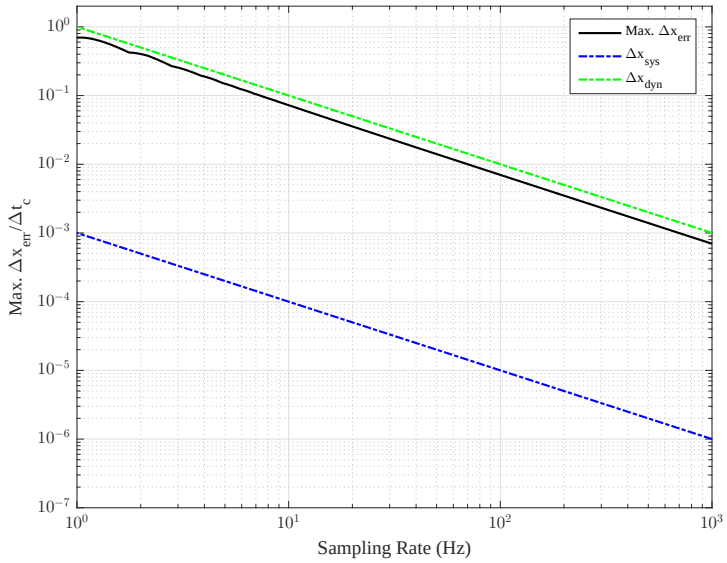

Figure 5. Maximum Change in Error During the Transient Phase for a SHO

Guidance Path Re-Planning Rates

The applicability of this metric is not only for the low-level controller as demonstrated, however, it can also be applied to the guidance, or path-planning, task as well. Since optimal control is predicated on a predictive model, uncertainty in the navigation solution, actuator dynamics, and unmodeled disturbances can degrade the quality of the solution over time and require an update to the problem. As a result, this metric can be used to estimate the rate at which it is necessary to generate a solution. To do so, however, requires the estimated error be bounded by some (error) function, e,

$$e \geq |f - \hat{f}| \tag{14}$$

where f is the dynamics of the system and $\hat{f}$ is the estimated dynamics of the system. Next, differentiating Eq. (14) with respect to time yields the error dynamics, $\dot{e}$. Note, the change in error over the real-time sampling period is,

$$\Delta e = \dot{e} T_{\text{RT}} \tag{15}$$

Substituting Eq. (15) into Eq. (6) as the change in position, one can solve for the time necessary to replan given the bounded error function e as,

$$T_{\text{RT}} = \frac{1}{2} \frac{\dot{e}}{\zeta_{\text{BW}}} \tag{16}$$

CONCLUSIONS

When implementing a controller for a physical system, the rate at which the system is sampled and controlled must be determined. Often times, this rate is chosen through various ”Rules of Thumbs” which are rooted in the frequency domain. However, a new approach to determine the minimum sampling rate rooted in first principles for the real-time control of a spacecraft was presented and validated via numerical case studies. This approach exploits the discrete nature associated with the digital implementation of a modern control system along with a unique view on the underlying

dynamics to derive an estimate for the minimum sampling rate necessary for a control system to be considered real-time. This metric, unlike other methodologies, is valid for both linear and nonlinear systems. Additionally, the resulting formulation easily maps to the physical system. Several case studies were performed using relevant linear and nonlinear systems including a spacecraft undergoing a 3-axis reorientation maneuver using an Eigenaxis-Quaternion feedback controller to a double integrator system under a minimum-time control policy. Each system considered utilized a realistic actuator with discrete output levels. From these case studies, the proposed metric was found to sufficiently estimate the average steady-state output of the system. Additionally, by exercising the flexibility of the definition *dynamic bandwidth*, an upper bound on the minimum sampling rate can be found by estimating transient tracking capabilities of the system. Furthermore, an extension of this metric was presented to estimate the rate at which the guidance path re-planning task must be performed. This metric, while does not exactly predict the necessary sampling rate, provides an estimate to well within an order of magnitude with few assumptions under ideal conditions.

ACKNOWLEDGMENT

The authors would like to acknowledge both Dr. Roberto Cristi and Dr. Josue Muñoz for their time, questions, and feedback, as this ultimately helped to refine the work presented.

APPENDIX: STABILITY OF A DOUBLE INTEGRATOR SYSTEM UNDER A MINIMUM-TIME OPTIMAL CONTROL POLICY

The dynamics of a double integrator system whose state $\mathbf{x} = [x_1, x_2]^{\mathrm{T}}$ can be written as,

$$\begin{aligned} \dot{x}_1(t) &= x_2(t) \\ \dot{x}_2(t) &= \frac{u(t)}{m} \end{aligned} \tag{17}$$

where m is the mass and $u(t) \in [u^-, u^+]$ is the admissible control input bounded by both a maximum negative and positive input limit. The resulting minimum time control policy to move a system from some initial condition to a desired terminal state,[10]

$$u^*(t) = \begin{cases} u^-_{\text{max}} & \text{for } s(\mathbf{x}(t)) > 0 \\ u^+_{\text{max}} & \text{for } s(\mathbf{x}(t)) < 0 \\ u^-_{\text{max}} & \text{for } s(\mathbf{x}(t)) = 0 \text{ and } x_2(t) > 0 \\ u^+_{\text{max}} & \text{for } s(\mathbf{x}(t)) = 0 \text{ and } x_2(t) < 0 \end{cases} \tag{18}$$

where the switching curve, $s(\mathbf{x}(t))$, is given as,

$$s\left(\mathbf{x}(t)\right) = x_1(t) + \frac{m}{2|u|}|x_2(t)|x_2(t) = 0 \tag{19}$$

For a non-zero T_s, maintaining the optimal *bang-bang* control policy would result in a limit cycle about the equilibrium point. In an effort to assess stability of the control policy off the switching curve, the optimal control policy in Eq. (18) is relaxed, allowing the control to vary continuously between $u^- \leq u \leq u^+$. Next, the control law for $s(\mathbf{x}(t)) \neq 0$ can be rewritten in terms of the dynamic bandwidth, ζ_{BW},

$$u(t) \approx -k\left(x_1(t) + \frac{1}{2\zeta_{\text{BW}}}|x_2(t)|x_2(t)\right) \tag{20}$$

where $k \in \mathbb{R}_+$ is a strictly positive constant converting the switching curve into a control input. For now, no other bounds will be imposed upon k. Lyapunov's Direct Method can be used to assess the stability of the candidate control law.

Consider the following positive-definite, energy-like Lyapunov candidate function (LCF),

$$V(\mathbf{x}) = \frac{1}{2}x_1^2 + \frac{1}{2}\lambda x_2^2 \tag{21}$$

where $\lambda \in \bar{\mathbb{R}}_+$ is a non-negative constant and has units of s^2. The time derivative of LCF along the system trajectory is,

$$\dot{V}(\mathbf{x}) = x_2(x_1 + \lambda \dot{x}_2) \tag{22}$$

Substituting the control law in Eq. (20) into Eq. (23) yields,

$$\dot{V}(\mathbf{x}) = x_1 x_2(1 - \lambda k) - \frac{\lambda k}{2\zeta_{\text{BW}}}|x_2|x_2^2 \tag{23}$$

When the trajectory of $\dot{V}(\mathbf{x})$ is in the vicinity of the origin such that $|x_2^3| << |x_1 x_2|$, the time derivative of the LCF can be simplified as,

$$\dot{V}(\mathbf{x}) \approx x_1 x_2(1 - \lambda k) \tag{24}$$

This simplification allows one to gain insight into the dynamics of the LCF.

First, for $0 < k < 1$, Quadrants II and IV, are 'stabilizing' as $\dot{V}(\mathbf{x}) < 0$ while Quadrants I and III are 'destabilizing' as $\dot{V}(\mathbf{x}) > 0$. This is illustrated by the contours of the full, nonlinear

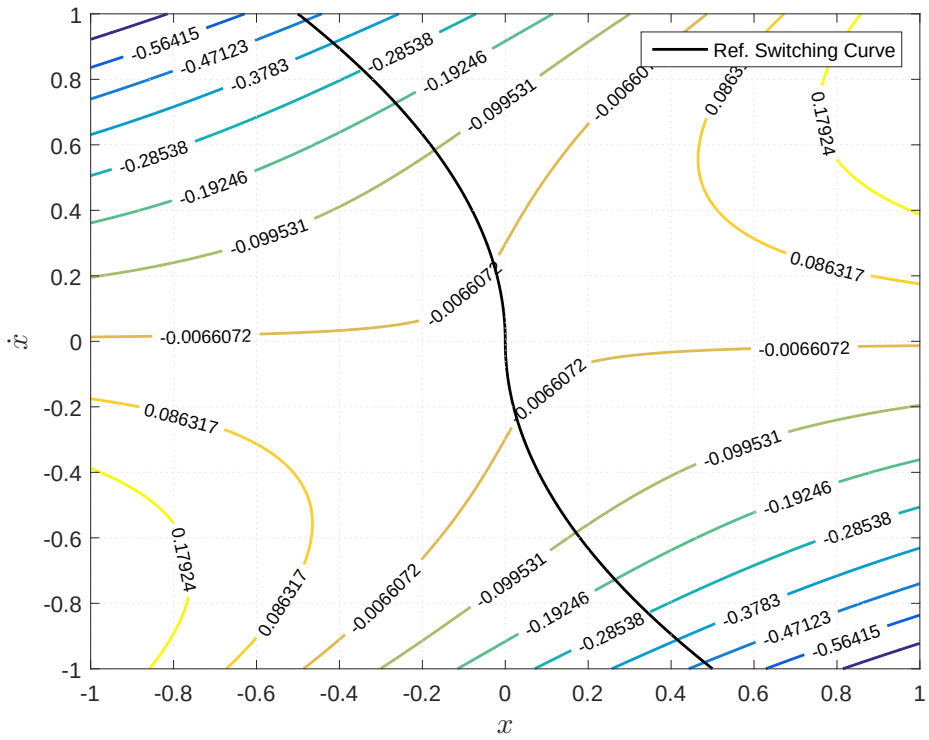

Figure 6. Contours of the $\frac{\partial V}{\partial t}$ for the Nonlinear LCF for $k = 0.5$ and $\lambda = 1$

time derivative of $V(\mathbf{x})$ is illustrated in Figure 6. In essence, when the trajectory $\mathbf{x}(t)$ moves into Quadrants I or III, the control law adds energy into the system to move it back into either Quadrant II or IV towards the switching curve in an effort to drivie the system towards the terminal state. For $k > 1$, the (de)stabilizing quality of each quadrant is reversed. Therefore, this implies the logical bound $k \in [0, 1)$.

REFERENCES

[1] M. C. Berg, N. Amit, and J. D. Powell, "Multirate digital control system design," *IEEE Transactions on Automatic Control*, Vol. 33, Dec 1988, pp. 1139–1150, 10.1109/9.14436.

[2] G. F. Franklin, J. D. Powell, and M. L. Workman, *Digital control of dynamic systems*, Vol. 3, ch. 3,10. Addison-wesley Menlo Park, 1998.

[3] K. Ogata, *Modern Control Engineering*, pp. 430—436, 439–440. Prentice-Hall, Inc, 1970.

[4] N. S. Nise, *CONTROL SYSTEMS ENGINEERING, (With CD)*. John Wiley & Sons, fifth ed., 2007.

[5] I. M. Ross, P. Sehavat, A. Fleming, and Q. Gong, "Optimal Feedback Control: Foundations, Examples, and Experimental Results for a New Approach," *Journal of Guidance, Control, and Dynamics*, Vol. 31, March-April 2008, pp. 307–321, 10.2514/1.29532.

[6] I. M. Ross, Q. Gon, F. Fahroo, and W. Kang, "Practical Stabilization Through Real-Time Optimal Control," *Proceedings of the 2006 American Control Conference*, Minneapolis, Minnesota, June 14-16 2006, pp. 304–309.

[7] I. M. Ross, *A Primer on Pontryagin's Principle in Optimal Control*, pp. 63–74. Collegiate Publisher, second ed., 2016.

[8] B. Wie, H. Weiss, and A. Arapostathis, "Quaternion Feedback Regulator for Spacecraft Eigenaxis Rotations," *Journal of Guidance, Control, and Dynamics*, Vol. 12, No. 3, 1989, pp. 375–380.

[9] B. Wie, *Space Vehicle Dynamics and Control*, pp. 349–362, 426–444. AIAA Education Series, second ed., 2008.

[10] D. E. Kirk, *Optimal Control Theory* An Introduction, ch. 5, pp. 248–259. Dover, 2004.